

The Modification Mechanism of Lanthanum Doping in Ti/Sb-SnO₂ Electrode and its Electrocatalytic Behavior of Degradation of *p*-nitrophenol

Qiang Bi*, Juanqin Xue, Changbin Tang, Lihua Yu, Guoping Li, Xiao Zhang

School of Metallurgical Engineering, Xi'an University of Architecture and Technology, Xi'an 710055, Shaanxi, China

*E-mail: bxqiang12@126.com

Received: 7 May 2016 / Accepted: 22 June 2016 / Published: 7 August 2016

Element doping is one of the effective means to improve the electrochemical performance of electrode. In order to improve the electrocatalytic performance of Ti/Sb-SnO₂ electrode, lanthanum was selected as a promoter to dop in the electrode coating. The micrograph and the structure of the electrode were characterized by SEM and XRD. Element composition of catalyst layer was determined by EDS. The electrochemical performance of Ti/Sb-SnO₂-La electrode was detected by electrochemical workstation. Doped and undoped electrodes were used to treat simulated *p*-nitrophenol (*p*-NP) wastewater. The electrochemical degradation efficiency of the two electrodes for treating *p*-NP was compared. The results showed that 92.8% *p*-NP was removed when using Ti/Sb-SnO₂-La as anode, which is much higher than that when using Ti/Sb-SnO₂ as anode. The effect of electrolytic parameters (electrolytic voltage, applied voltage, electrode distance, electrolyte concentration and pH value) on *p*-NP degradation were also studied. On the basis of electric catalytic oxidation mechanism, the degradation mechanism of *p*-NP was deduced. According to the experimental results, the electrocatalytic performance of the La doped electrode was superior for the treatment of *p*-NP wastewater.

Keywords: Ti/Sb-SnO₂-La electrode, electrocatalytic, rare earths, *p*-NP wastewater

1. INTRODUCTION

With the development of organic synthesis industry, more and more refractory organic pollutants are discharged into wastewater, most of which are either carcinogenic or teratogenic material. However, the traditional biological degradation technology for wastewater treatment can't reach the increasingly strict environmental protection requirements. Recently, advanced oxidation processes (AOPs) have been proposed to treat the non-biodegradable industrial wastewater[1-4]. Most AOPs require severe reaction conditions such as high temperature and pressure, or need to use noble

metal catalysts such as Pt and Rh[5,6]. Electrochemical oxidation technology is cost-effective, easy to apply and effective for relatively low-strength wastewater containing organic compounds and has been attended and regarded as an environmental friendly technology [7-10].

In electrochemical oxidation process, due to the special interface properties between electrode and solution, a lot of reactions which are not able to occur or need harsh conditions can perform under normal temperature and pressure. Various electrodes have different oxidation capacity for organic pollutants, and the electric catalytic oxidation performance of most electrodes is not ideal. Boron doped diamond electrode has good catalytic property, but expensive production cost limits its application[11,12]. According to current studies, Ti/SnO₂ is a promising dimensionally stable anode in wastewater treatment due to its high cost performance[13,14]. The Ti/SnO₂ doped with Sb has been widely used in all kinds of wastewater treatment research as high efficient electrode, but its catalytic oxidation performance and service life has not reached the level of industrial application[15,16]. Therefore, the systematic study of the relationship between electrochemical oxidation performance and modification methods of electrode has important theory significance and practical value.

The electrochemical oxidation performance of electrode can be highly improved as doped with metal element[17,18]. Owing to their special structure of 4f electronic shell, rare earth elements have particular physical and chemical properties. And they had been extensively used in optics, electrics, and magnetics, and had played a very important role in functional materials[19-21]. A lot of researchers now try to dope rare earth elements into electrode activation layer to improve its electrochemical oxidation performance. Most researches focused on the preparation and characterization of electrode, but the modification mechanism and application of electrode was ignored[22, 23].

In this paper La doped Ti/Sb-SnO₂ electrode was prepared in two different ways and their performances were compared. Modification mechanism of La doped Ti/Sb-SnO₂ electrode was discussed according to the analysis of electrode by SEM, XRD, EDS, XPS and LSV. The influences of electrolytic process conditions on the electrochemical oxidation performance were investigated by treating simulated *p*-NP wastewater, and the suitable doping ratio of La was confirmed.

2. EXPERIMENTAL

2.1 Preparation of the electrocatalytic electrodes

2.1.1 Materials

All chemicals used in the experiment were of analytical grade and employed without any further purification. Ti substrate was offered by Xi'an metal company. Working solutions of samples were prepared by *p*-NP with Milli-Q grade water.

2.1.2 Preparation of Ti substrate

Ti substrate with a dimension of 50mm×30mm was polished by 180, 600 and 1000 mesh abrasive papers, until Ti substrate presented a metallic luster. After degreased using 10% sodium hydroxide solution, Ti substrate was etched in boiling oxalic acid (10%, m/m) for 2 hours to produce a gray surface with uniform roughness.

2.1.3 Preparation of electrode coating

The SnO₂ coated Ti electrodes were prepared by the following two methods.

1) Immersion method

The electrodes were prepared by immersion method as described in Ref. [24, 25]. Certain amounts of SnCl₄·5H₂O, Sb₂O₃ and La₂O₃ were dissolved in HCl aqueous solution and then some ethanol was added to obtain the electrocoating solution. The mole ratio of Sn to Sb was 100:10. Ti substrate was soaked into the solution for 1 min, dried in oven at 120 °C, and then heated at particular temperature for 15min, followed by cooled in room temperature. The operation was repeated 15 times to produce a qualified La doped Ti/Sb-SnO₂ electrode, and the last baking was annealed for 2 h at 500 °C.

2) Sol-gel method

The electrodes were prepared by sol-gel according to the method in Ref. [26, 27]. First, certain amount of SnCl₄·5H₂O, Sb₂O₃ and La₂O₃ were dissolved in HCl aqueous solution, ethylene glycol were mixed with this solution and agitated at 60°C until full dissolution; then the solution was heated to 90°C with continuous stirring. After that, the solution was maintained at 90°C for 30 min to obtain sol-gel. Finally, the sol-gel solution was applied on Ti substrate by brushing, drying and thermal decomposition. The whole process was repeated 15 times to produce the Ti/Sb-SnO₂-La electrode, and the last baking was annealed for 2 h at 500 °C.

The methods for preparation of Ti/SnO₂, Ti/Sb-SnO₂, Ti/Sb-SnO₂-La electrodes were the same except that the solution compositions varied for different electrodes. The influence of doping ratio of La to Sn and the heat treatment temperature on the performance of Ti/Sb-SnO₂-La electrode was investigated in this work.

2.2. Instrument analysis

The crystal phase identification and determination of the crystallite size of the SnO₂ were analyzed by X-ray diffraction (XRD, PHI-5400) using Cu K α radiation. The microstructures were examined using a scanning electron microscope (SEM, JSM-7600F) in back-scattered electron mode.

The electrochemical behaviors of electrodes were tested with standard three electrodes cell (PARSTAT-2273). The self-designed electrodes (Ti/SnO₂, Ti/Sb-SnO₂, Ti/Sb-SnO₂-La) were used as the working electrode, a platinum sheet as the counter electrode and a saturated calomel electrode as the reference-electrode. The apparent oxygen evolution potentials of the electrodes were obtained by linear sweep voltammetry (LSV) electrochemical tests in 0.5M H₂SO₄ [26, 28].

2.3 Experiment of electrocatalytic oxidation

Bulk oxidations were performed in an undivided electrochemical cell of 0.2 L (Fig. 1). The self-designed electrodes by sol-gel method were employed as anode, and a titanium plate was utilized as cathode. The electrodes are rectangle and each of them had a geometric area of 15 cm². Electrochemical oxidation experiments were accomplished at 25°C. In the case of the mediated oxidation process, experiments were performed by varying the Na₂SO₄ concentration in solution (0.3, 0.4, 0.5, and 0.6 mol·L⁻¹ in 0.15 L of solution containing *p*-NP).

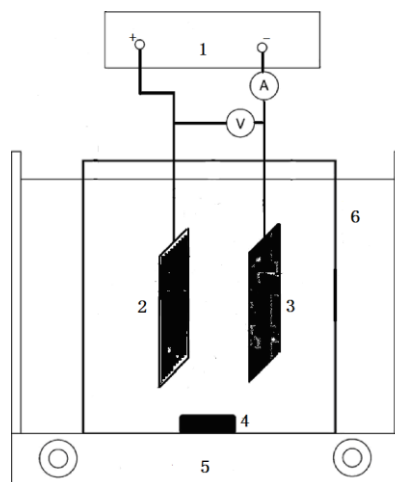


Figure 1. Schematic diagram of experimental setup; 1: power supply; 2: anode; 3: cathode; 4: magneton 5: magnetic stirrer; 6: thermostat water bath.

2.4 Analyzing the intermediates produced during *p*-NP degradation

The reaction intermediates of the treated water at different time were investigated by ultraviolet spectrophotometry (TU-1901) from 190nm to 900nm. The possible degradation mechanism of *p*-NP was deduced from the UV spectra at different electrolysis time.

3. RESULTS AND DISCUSSION

3.1 Preparation process optimization of La doped Ti/Sb-SnO₂

3.1.1 Performance of *p*-NP degradation by different anodes

The pollutant degradation effect in electrochemical oxidation process was mainly determined by the electrodes. Fig. 2 shows the performance of *p*-NP degradation by different anodes. As shown in Fig. 2, the *p*-NP concentrations decreased by 50.6%, 59.6%, 68.9% and 92.8% on Ti sheet, Ti/SnO₂, Ti/Sb-SnO₂, and Ti/Sb-SnO₂-La anodes, respectively, at an initial 100 mg/L *p*-NP concentration at a constant voltage of 12 V with a 0.5mmol/L Na₂SO₄ supporting electrolyte solution in 120 min. The results were in good agreement with the results reported by Cui [29].

The electrochemical oxidation ability of the electrode materials depend on electron transfer rate and hydroxyl radical generation quantity in the electrochemical reaction process. The results suggested Ti/Sb-SnO₂-La anodes exhibited good electron transfer capacity and could produce large amount of hydroxyl radical. The higher electrocatalytic performance of Ti/Sb-SnO₂-La than others may be due to two factors. First, La extruding into the crystal lattice by way of replacement, filling gap, or dispersion, increased the activity sites of the electrodes. In addition, the doped La may change the distribution of energy band of SnO₂ and form deeper energy band.

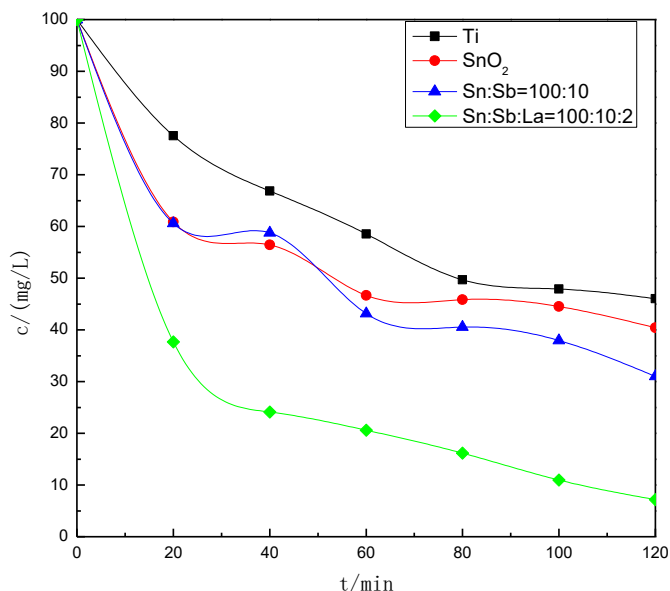


Figure 2. Performance comparisons of different anode materials (*p*-NP concentration:100 mg/L, heat treatment temperature: 500°C, preparation of electrode coating: sol-gel method)

3.1.2 The effect of preparation methods on electrode performance

Fig. 3 shows the degradation effects of *p*-NP under the same conditions by two kinds of electrode which prepared with immersion and sol-gel methods, respectively. It could be deduced from Fig. 3 that the electrocatalytic performance of the electrode prepared by sol-gel method is better than the electrode prepared by immersion method, the degradation efficiency of *p*-NP is 92% and 70% by the above anodes electrolyzing for 120min, respectively.

This consequence was mainly attribute to that in the process of preparing electrode by sol-gel method, brushing function can make coating is compact and uniform and components distribute uniform. After the repeating brushing process, the mandatory mechanical effect was strengthened. According to the literature, the oxygen species in the electrode coating prepared by sol-gel method mostly is adsorption oxygen, this is benefit to the directly mineralization of pollutants[30]. Therefore, this electrode has better electrocatalytic oxidation performance.

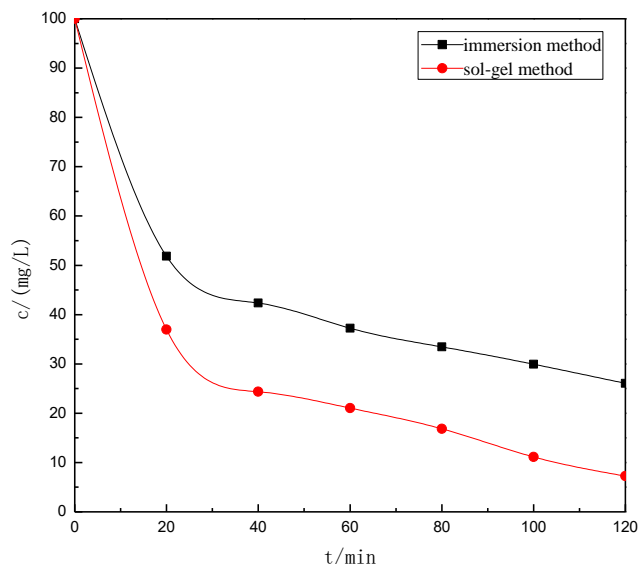


Figure 3. The effect of preparation method on electrode performance (*p*-NP concentration:100 mg/L, heat treatment temperature: 500°C, Sn: Sb: La =100:10:2)

3.1.3 The effect of heat treatment temperature on electrode performance

In the preparation process of electrode, heat treatment temperature as the crucial factor will directly influence the coating grain nucleating, growing rate and phase structure of lattice, and then influence the catalytic activity, real surface area and longevity of the electrode coating. Fig. 4 shows the degradation result of *p*-NP by Ti/Sb-SnO₂-La (mole ratio Sn: Sb: La=100: 10: 2) electrodes which treated at different temperature. As shown in Fig. 4, the electrocatalytic performance of the electrode treated at 500°C was the best. This conclusion agrees well with the other results [31, 32].

With the increase of heat treatment temperature, the solid solubility of Sb, Sn and La as their mutual diffusion was enhanced; consequently, the adhesion of coating and Ti substrate was strengthened. At the higher heat treatment temperature, more SnO₂ grains formed in the coating, so the electrocatalytic performance of electrode was superior. However, SnO₂ grains are coarsened at the exceedingly high treatment temperature, the number of grains are decreased at the same axis direction, this led to the electrocatalytic performance was deteriorated.

At the too higher treatment temperature, the coating will be over oxidized and then the rutile structure of SnO₂ will be destroyed, meanwhile Sb₂O₃ will be loss as evaporation, coating composition will be changed. Ti substrate will form passivation layer with the over oxidation at excessive treatment temperature, so electrode conductivity will decline. The passivation layer will reduce the adhesion strength of the substrate and oxide layer, and then curtail the longevity of electrode. So in the following electrode preparation experiment the heat treatment temperature was maintained at 500°C.

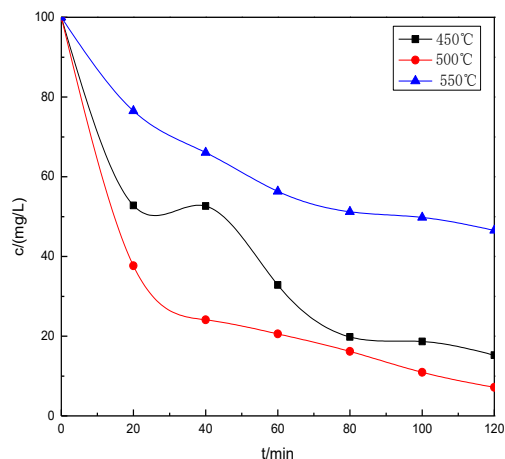


Figure 4. The effect of heat treatment temperature on electrode performance (*p*-NP concentration:100 mg/L, Sn: Sb: La =100:10:2, preparation of electrode coating: sol-gel method)

3.1.4 The effect of La doping amount on electrode performance

Fig. 5 shows the degradation efficiency of *p*-NP by using the Ti/Sb-SnO₂-La anodes prepared with different La doping amount. As can be seen from Fig. 5, the degradation efficiency of *p*-NP is the highest on the anode elements mole ratio Sn: Sb: La is 100: 10: 2. This is because more La doping amount caused more defects in the coating like voids and vacancies, and enhanced the electrocatalytic performance of electrode. However, the electrode displayed a poor electrocatalytic performance with the doping amount excess increases.

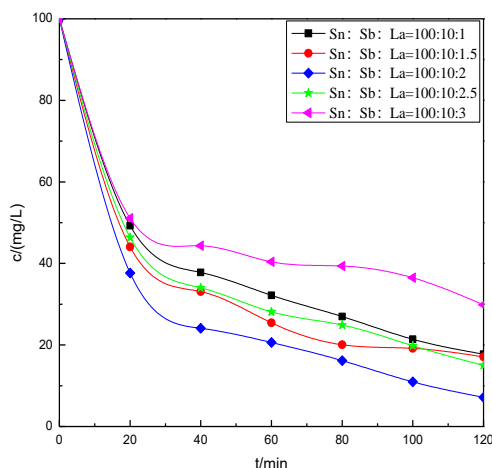


Figure 5. The effect of La doping amount on electrode performance (*p*-NP concentration:100 mg/L, heat treatment temperature: 500°C, preparation of electrode coating: sol-gel method.)

With La doping amount increased to a certain value, due to point defect became the combined center of electron-vacancy, the combining odds of electron-vacancy was added; at the same time, Sb atoms could display Sn atoms in the SnO₂ lattice. The two points led to the destruction of SnO₂ lattice

and the increase of lattice disorder, so the effective components in the coating would precipitate out as impurities and then the electrocatalytic performance of electrode is poor. Therefore, the elements mole ratio Sn: Sb: La is 100: 10: 2 in the subsequent electrode preparation experiment.

3.2 Characteristic of electrode

3.2.1 SEM and EDS analysis

The morphology of three electrodes including Fig. 6 (a) Ti/SnO₂, (b) Ti/Sb-SnO₂ and (c) Ti/Sb-SnO₂-La were observed by using scanning electron microscope (SEM). As shown in Fig. 6, all electrodes coating are in “crack mud” shape, there are different degrees of cracks in electrode surface. It can be observed clearly from Fig. 6 (a) and (b) that the cracks in undoped electrode surface are deeper and more than that on doped one. The coating with badly formed lattice is uneven. Too many cracks accelerated oxidation process of Ti substrate and reduced the bonding force between coating and Ti substrate. There is a slight and shallow rimous pattern on the surface of Ti/Sb-SnO₂-La electrode. Duo to uniform high-density little pieces structure, electrode coating has large roughness and specific surface area, and has good electrical conductivity and catalytic performance.

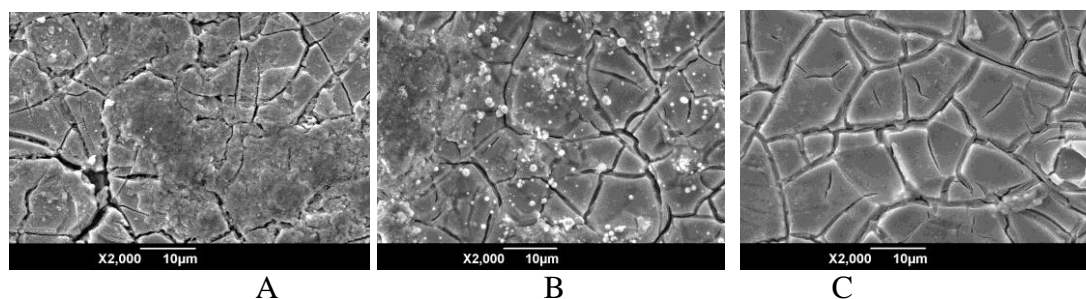


Figure 6. SEM of the electrodes, A: Ti/SnO₂; B: Ti/Sb-SnO₂; C: Ti/Sb-SnO₂-La (Sn: Sb: La =100:10:2, heat treatment temperature: 500°C, preparation of electrode coating: sol-gel method)

Table 1. EDS test result of electrode (2% La + Ti/Sb-SnO₂) coating

Element	keV	Atom%
Sn L	3.442	24.69
Sb L	3.603	7.44
La L	4.648	0.85
Cl K	2.621	1.13
Al K	1.486	3.61
O K	0.525	62.28
Total		100.00

The elements in the electrode coating were detected by EDS, the result is showed in Tab. 1. In 2% La doped Ti/Sb-SnO₂ electrode coating, the test values of Sn, Sb and La is 100:30:3(mole ratio). It can be concluded that La and Sb in the coating are not involved in nucleation, they enrich in SnO₂ grain crevices and detail the grain.

3.2.2 XRD analysis

Fig.7 shows the X-ray diffraction (XRD) patterns of three electrodes including (a)Ti/SnO₂, (b) Ti/Sb-SnO₂ and (c) Ti/Sb-SnO₂-La. As shown in Fig. 7, three electrodes all have obvious diffraction peaks at $2\theta=(26.6^\circ, 33.7^\circ, 51.9^\circ)$, according to the PDF number: 00-044-129, which can be indexed as the (1 1 0), (1 0 1) and (2 1 1) diffraction peaks of SnO₂. In the XRD pattern of (b) and (c), only SnO₂ is found no Sb and La is observed, because Sb and La present in a very small amount . It can be seen from Fig. 7 (c) that the diffractive peaks became wider by doping La into coating. According to literature [30], the diffraction peak width is inversely proportional to crystallite size. The result indicates that the La doped electrode coating has smaller crystallite size than the undoped coating, which is also confirmed by SEM images [30].

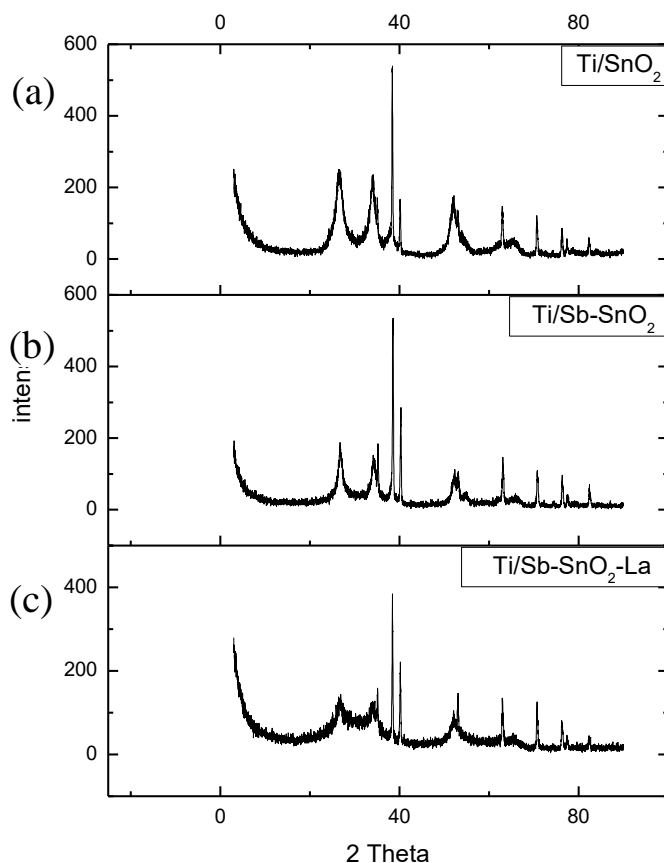


Figure 7. XRD patterns of the electrodes, a: Ti/SnO₂, b: Ti/Sb-SnO₂, c: Ti/Sb-SnO₂-La (Sn: Sb: La =100:10:2, heat treatment temperature: 500°C, preparation of electrode coating: sol-gel method)

3.2.3 XPS analysis

Fig. 8 shows the X-ray photoelectron spectroscopy (XPS) patterns of three electrodes, Fig. 8(a) shows the XPS patterns of Sn 3d, at the vicinity of 486 eV the binding energy absorption peak belongs to Sn 3d_{5/2}, and absorption peak of Sn 3d_{3/2} appears near the 496 eV [29, 33]. As shown in Fig. 8(a), the Sn 3d binding energy of Ti/Sb-SnO₂-La electrode is least. It illustrates that in La doped electrode coating, the average electron cloud density around of Sn⁴⁺ is higher than other electrode.

SnO₂ is a stoichiometric compounds, higher average electron cloud density means that in the electrode coating lattice oxygen content is less, while oxygen vacancies are more. The catalytic activity of semiconductor mainly depends on the existence of oxygen vacancy, it may be beneficial to the generation of hydroxyl radicals. The doping of rare earth La increased the oxygen vacancy in electrode coating, and then promoted the generation of hydroxyl radicals in electrochemical reaction process.

Fig. 8(b) shows the XPS patterns of O 1s, the binding energy absorption peak of O 1s is sharper and less overlapping. This illustrates that in the doped electrode coating the oxygen species is relatively single, and absorption peak appears the 531 eV that shows it is mainly chemical adsorption oxygen. The absorption peak area of La doped electrode is the biggest, that indicates doping obviously increased adsorption oxygen quantity.

As shown in Fig. 8, XPS analysis demonstrated that the electrocatalytic activity of the La doped electrode is better than the others. The actual degradation efficiency of *p*-NP by three electrodes as shown in Fig.2 confirmed this.

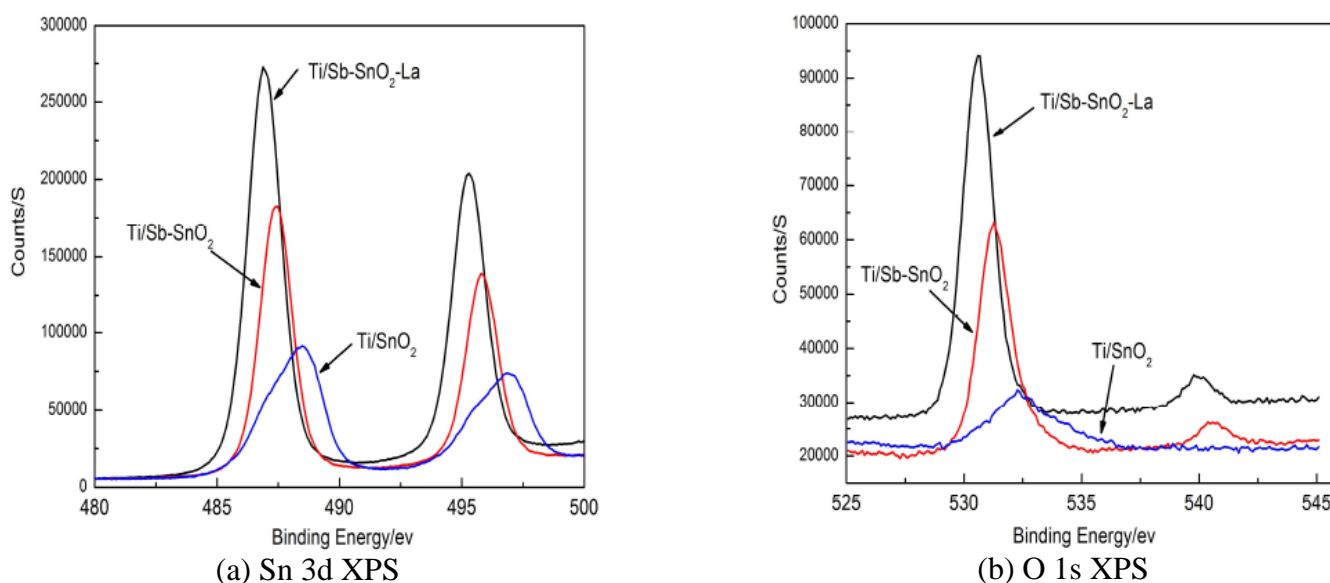


Figure 8. XPS patterns of different electrodes (Sn: Sb: La =100:10:2, heat treatment temperature: 500°C, preparation of electrode coating: sol-gel method)

3.2.4 LSV analysis

Oxygen evolution reaction is the main side effect in the process of electrochemical oxidation degradation on organic pollutants, and the over potential for oxygen evolution determines the difficulty and amount of oxygen evolution reaction. In order to reduce the side effects and improve the degradation efficiency of electrochemical oxidation process, the electrode with high oxygen evolution potential need to be prepared. Fig. 9 shows the LSV curves of different electrodes.

As shown in Fig.9, According to the literature[26, 34-35], the red line is the tangent with LSV curve, through the auxiliary line in the graph, the oxygen evolution potential of three electrodes Ti/SnO₂, Ti/Sb-SnO₂ and Ti/Sb-SnO₂-La is 1.54V, 1.62V and 1.74V, respectively.

The results of LSV analysis indicated that La doped in electrode coating improved the oxygen evolution potential. In the progress of electrochemical processing wastewater, La doped electrode manifested the inhibition of oxygen evolution reaction, and this improved the degradation efficiency of wastewater. Grain refining and density surface will reduce the adsorption of groups that produce oxygen evolution reaction on the electrode, the adsorption effect of the group is the dominant factor decided the oxygen evolution potential [34].

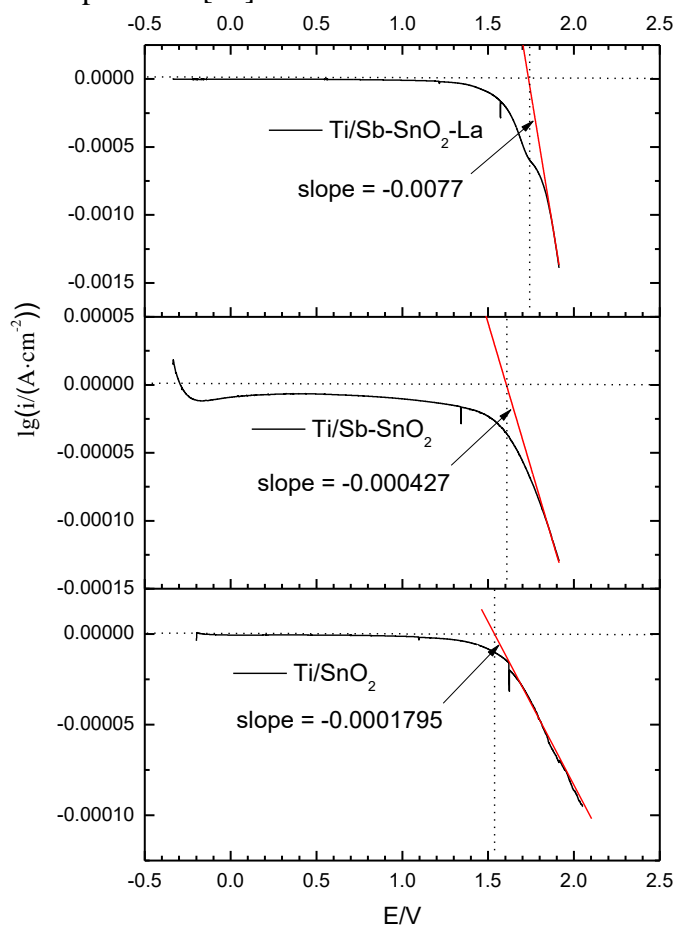


Figure 9. Anodic polarization curves of Ti/SnO₂, Ti/Sb-SnO₂, Ti/Sb-SnO₂-La (0.5 M H₂SO₄, potential range: -0.5 ~ 2.0 V vs. SCE, scan rate: 10 mV s⁻¹)

3.3 Influence of operating variables on electrocatalytic performance

3.3.1 Influence of electrolytic time on *p*-NP removal rate

As shown in Fig. 10, the concentration of *p*-NP decreased constantly with the increase of electrolytic time, and reached at 8% after 120 min. In the early 40 min, the concentration dropped rapidly, this is due to in the initial stages of electrolysis process the high concentration *p*-NP can quickly spread to the electrode surface and be degraded. The same electrolytic process was reported in the literature [28, 36].

With most of the *p*-NP were oxidized, fewer amount of *p*-NP diffuse to the electrode surface. Furthermore, the intermediates during the *p*-NP degradation increased as time expend, they can be degraded further by reacting with $\cdot\text{OH}$, and then the competing reactions of *p*-NP degradation increased.

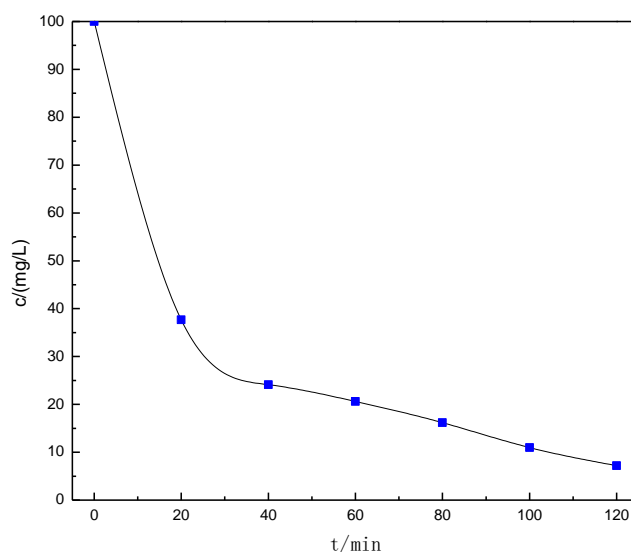


Figure 10. Influence of electrolytic time on *p*-NP removal rate (cell voltage: 12V, electrode distance:25mm, Na_2SO_4 concentration: 0.5mol/L, pH:6-7)

3.3.2 Influence of cell voltage on *p*-NP removal rate

The capability of electron transfer and hydroxyl radical generation may govern the degradation efficiency of *p*-NP in aqueous solution. However, the above abilities, especially hydroxyl radical generation capability depend on the applied voltage. Hence the effect of applied voltage on the degradation rates of *p*-NP (100 mg/L) was investigated by setting the voltage of 6, 8, 10, 12, 14 and 16 V.

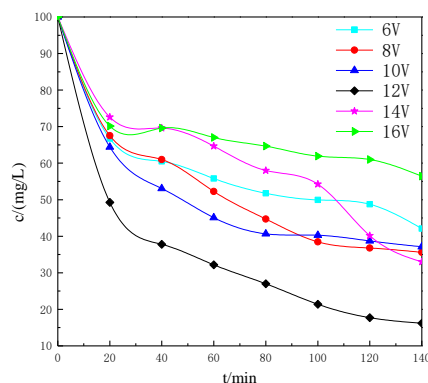
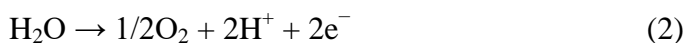


Figure 11. Influence of cell voltage on *p*-NP removal rate (electrode distance:25mm, Na₂SO₄ concentration: 0.5mol/L, pH=6-7)

It could be deduced from Fig. 11 that the degradation rate of *p*-NP increased first and decreased afterwards with the increasing applied cell voltage, and the degradation rate of *p*-NP was the highest at applied voltage 12v. The results agree well with the document [36]. This behavior can be attribute to that the driving force of degradation reaction was enhanced and the generation of hydroxyl radical was accelerated with the increasing applied cell voltage. It has been proposed that $\cdot\text{OH}$ radicals formed by water oxidation (Eq. (1)). Higher voltage is benefit for Eq. (1), however, over high voltage could bring to the side reaction of oxygen evolution (Eq. (2)) [37]. The side reaction at over high voltage decreased the amount of hydroxyl radical in the solution, and then the degradation of *p*-NP was reduced.



3.3.3 Influence of electrode distance on *p*-NP removal rate

As shown in Fig. 12, the *p*-NP removal ratio increased first and then decreased with expanding of electrode distance. The hydroxyl radical generated on anode could easy happen reduction action on cathode while never react with *p*-NP with too small plate distance. In addition, duo to smaller electrode distance, the water between of two electrodes could be churned by the bubbles generated in electrolytic process.

The adsorption quantity of organic pollutants on electrodes decreased because of the violent fluctuation of electrolyte. Therefore, the *p*-NP removal ratio was lower with smaller electrode distance. With the increase of electrode distance, the adsorption efficiency between electrodes and organic pollutants was enhanced, and the charge transmitting between them was more conveniently, as a result the *p*-NP removal ratio was increased accordingly. Nevertheless, if the electrodes were placed further apart, the cell voltage would rise sharply, and then the side reaction such as oxygen evolution reaction and hydrogen evolution reaction increased and degradation efficiency decreased.

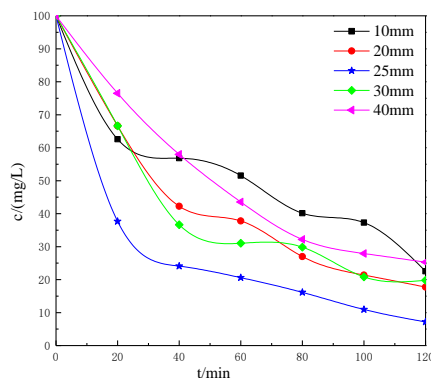


Figure 12. Influence of plate distance on *p*-NP removal rate (cell voltage: 12V, Na_2SO_4 concentration: 0.5mol/L, pH=6-7)

3.3.4 Influence of electrolyte (Na_2SO_4) concentration on *p*-NP removal rate

The electrical conductivity of solution would seriously influence the electrolyte efficiency of organic pollutants in electrochemical systems. Fig. 13 shows the effect of Na_2SO_4 as the electrolyte on *p*-NP degradation ratio. As shown in Fig. 13, at first, *p*-NP degradation ratio increased with the increase of Na_2SO_4 .

This is due to the electrical conductivity of solution increased and the electron transfer speed was accelerated with the increase of interaction between electrolyte ion. At the same time with increase of the ions concentration, the collision probability of particles in the solution increased and this accelerated the degradation reaction rate. However, this effect was not unlimited, excessive concentration of Na_2SO_4 can lead to most adsorption of SO_4^{2-} on electrode surface. The adsorption and degradation of *p*-NP on the electrodes was prevented and the productivity of hydroxyl radical decreased duo to the adsorption of SO_4^{2-} .

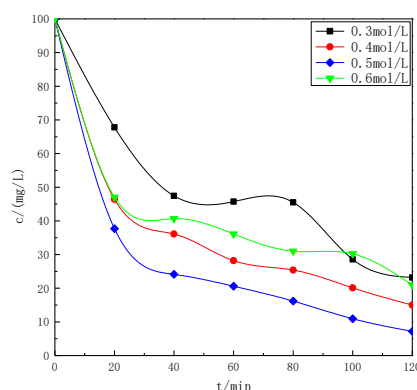


Figure 13. Influence of electrolyte concentration on *p*-NP removal rate (cell voltage: 12V, electrode distance: 25mm, pH: 6-7)

3.3.5 Influence of initial pH values on *p*-NP removal rate

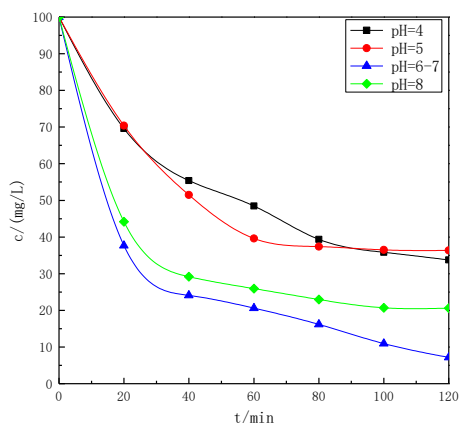


Figure 14. Influence of electrolyte concentration on *p*-NP removal rate (cell voltage: 12V, electrode distance: 25mm, Na₂SO₄ concentration: 0.5mol/L)

The initial pH value is an important parameter influencing the performance of the electrochemical process. Fig. 14 shows the effect of initial pH values on the *p*-NP degradation efficiency. As shown in Fig. 14, the degradation rate at initial pH value of 7 reach the highest level.

This behavior was mainly attributed to that the increase of the *p*-NP solution pH decreased the hydroxyl radical generation. However, it is interesting to observe that *p*-NP degradation rate decreased again under strong acidic conditions (pH = 4). The pH value can influence the existing form *p*-NP and residues. *p*-NP can not be dissociated at low pH, thus weakening the electromigration mass transfer. Furthermore, at low pH value, there are a great quantity SO₄²⁻ in the solution, they can impede the adsorption of *p*-NP on electrode. Consequently, the solution pH value can be kept at neutral as using electrochemical process to degradate *p*-NP wastewater.

3.4 Deducing *p*-NP degradation mechanism

The UV spectra of the treated water at different time was investigated, and used to deduce the degradation mechanism like other documents [36, 38-39]. As shown in Fig. 15, the absorption peak at 227 nm and 320 nm can be attributed to the characteristic absorption of *p*-NP. The absorption peak of 320nm weakens gradually with the increase of reaction time. Illustrating that the electronic conjugated system between benzene and auxochromic group (-NO₂) was destroyed. In other words, nitro dropt from benzene and benzene ruptured. The two absorption peaks are all disappear after 120 min, indicating that *p*-NP can be totally degraded by single electrochemical treatment.

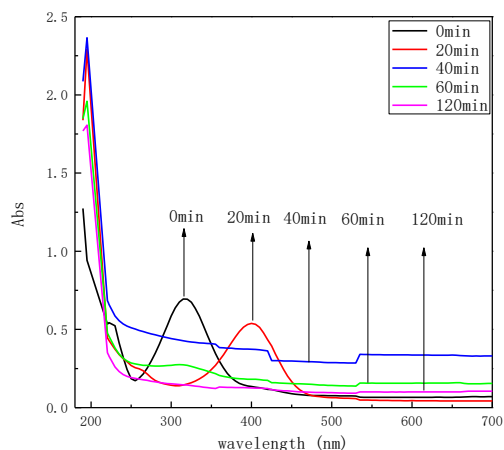


Figure 15. UV-vis spectra during the electrochemical degradation of *p*-NP

Combined with literature [36, 39, 40], the degradation process of *p*-NP was deduced as three steps, showed in Fig. 16. (I) First, nitro dropt from benzene, meanwhile the hydroquinone produced. Duo to the strong oxidation of hydroxyl radical, the hydroquinone easy be oxidized to benzoquinone rapidly; furthermore, hydroquinone can react with hydroxyl radical countinue and change into 1, 2, 4, - three hydroxy benzene. (II) Secondly, polyhydroxy-benzene and benzoquinone were degraded into organic acids by ring opening reaction, this is attributed that the hydrogen ions at ortho-position or para-position of benzene ring would be attacked by hydroxyl radical, ring opening reaction occurred and some small molecule organic acid such as formate, acetate and oxalate generated. (III) At last, organic acid was degraded into CO₂ and H₂O, so far, organic pollutants were completely mineralized.

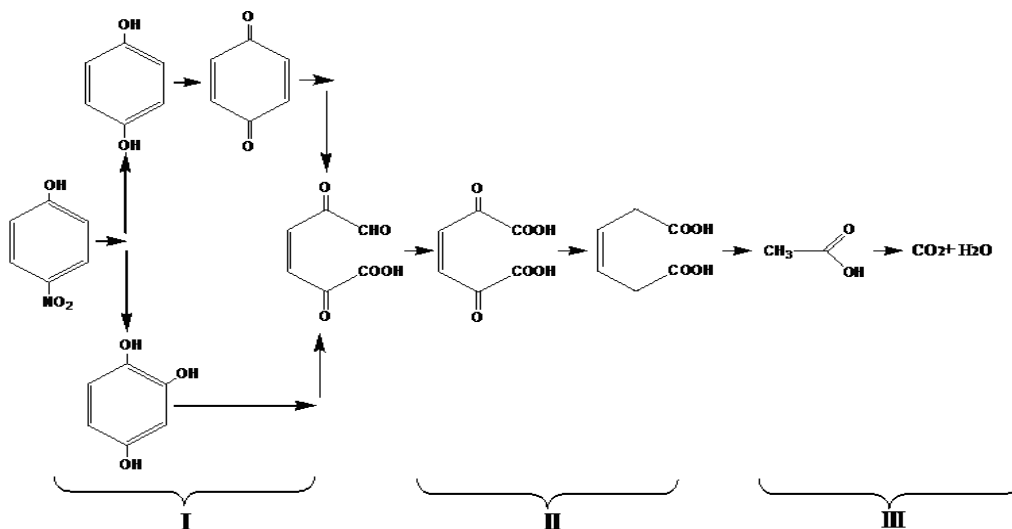


Figure 16. The degradation progress of *p*-NP

4. CONCLUSION

Sol-gel is a better method to prepare La doped Ti/Sb-SnO₂ electrode, and the catalytic performance of electrode which prepared at head treatment temperature 500°C and mole ratio Sn: Sb: La=100:10:2 in the coating was superior for the treatment of *p*-NP wastewater. The doped La may extrude into the crystal lattice by way of replacement, filling gap, or dispersion, it led to lattice expansion and charge unbalance and made voids and vacancies forming in electrode coating, therefore the catalytic oxidation ability of electrode was promoted. The electrochemical degradation of simulated *p*-NP wastewater was investigated. It can be concluded that when the applied voltage was 12V, plate distance was 25 mm, electrolyte concentration was 0.5mol/L and initial pH was 7, the *p*-NP removal rate can reach 92.8% in 120 min under mild conditions. It means that La doped in electrode coating was an efficient means to enhance its electrochemical performance and La doped Ti/Sb-SnO₂ electrode was a superior anode for treating *p*-NP wastewater.

ACKNOWLEDGEMENTS

The authors would like to acknowledge the support of the National Natural Science Foundation of China (51278407, 51408468), Shaanxi Provincial Department of Education Project (14JK1434).

References

1. W. P. Zhu, Y. J. Bin, Z. H. Li, *Wat. Res.* 8 (2002) 1947- 1954.
2. J. Zhang, S. Z. Wang, Y. Guo, *J. Environ. Sci.* 8 (2013) 1583-1591.
3. W. Gong, X. Duan, *Waste Manage.* 8 (2010) 2103-2107.
4. Z. L. Xiong, X. Cheng, D. Z. Sun, *J. Environ. Sci.* 5 (2011) 725-730.
5. K. H. Kim, S. K. Ihm, *J. Hazard. Mater.* 186 (2011) 16-34.
6. G. L. Qiu, Y. H. Song, P. Zeng, S. H. Xiao, *L. Chemosphere* 84 (2011) 241-246.
7. V. Francisca, C. Moreira, J. Soler, A. Fonseca, I. Saraiva, R. A. R. Boaventura, E. Brillas, V. J. P. Vilar, *Appl. Catal., B* 182 (2016) 161-171.
8. F. Sopaj, M. A. Rodrigo, N. Oturan, F. I. Podvorica, J. Pinson, M. A. Oturan, *Chem. Eng. J.* 262 (2015) 286-294.
9. M. A. M. Cartaxo, C.M. Borges, M.I.S. Pereira, M.H. Mendonça, *Electrochim. Acta* 176 (2015) 1010-1018.
10. W. Ma, Z. H. Cheng, Z. X. Gao, R. Wang, B. D. Wang, Q. Sun, *Chem. Eng. J.* 241 (2014) 167-174.
11. F. L. Souza, C. Saéz, M. R. V. Lanza, P. Cañizares, M. A. Rodrigo, *Electrochim. Acta* 187 (2016) 119-124.
12. H. Rubí-Juárez, S. Cotillas, C. Sáez, P. Cañizares, C. B. Díaz, M. A. Rodrigo, *Appl. Catal., B* 188 (2016) 305-312.
13. D. Shao, J. D. Liang,, X. M. Cui, H. Xu, W. Yan, *Chem. Eng. J.* 244 (2014) 288-295.
14. F. Chen, S. C. Yu, X. P. Dong, S. S. Zhang, *J. Hazard. Mater.* 227-228 (2012) 474- 479.
15. H. Lin, J. F. Niu, S. Y. Ding, L. L. Zhang, *Wat. Res.* 46 (2012) 2281-2289.
16. I. Pikaar, R. A. Rozendal, Z. G. Yuan, J. Keller, K. Rabaey, *Wat. Res.* 45 (2011) 5381-5388.
17. Q. Z. Dai, J. Z. Zhou, X. Y. Meng, D. L. Feng,, C. Q. Wu, J. M. Chen, *Chem. Eng. J.* 289 (2016) 239-246.
18. I. Cesarino, R. P. Simões, F. C. Lavarda, A. B. Neto, *Electrochim. Acta* 192 (2016) 8-14.

19. M. H. M. T. Assumpc, A. Moraes, R. F. B. Souza, I. Gaubeur, R. T. S. Oliveira, V. S. Antonina, G. R. P. Malpass, R. S. Rocha, M. L. Calegaro, M. R. V. Lanza, M. C. Santos, *Appl. Catal. A* 411-412 (2012) 1- 6.
20. Y. H. Song, G. Wei, R. C. Xiong, *Electrochim. Acta* 52 (2007) 7022-7027.
21. G. C. Han, Z. Liu., Y. L. Wang, *J. Rare Earth*, 26 (2008) 532-537.
22. F. Deganello, L. F. Liotta, S. G. Leonardi, G. Neri, *Electrochim. Acta* 190 (2016) 939-947.
23. Y. H. Cui, Y. J. Feng, Z. Q. Liu, *Electrochim. Acta* 54 (2009) 4903-4909.
24. S. P. Li, Z. Hu, H. L. Cao, *J. Chin. RE. Soc.* 26 (2008) 291-297.
25. S. P. Li, J. Fu, Z. Hu, *J. Shandong Univ.* 43 (2008) 22-26.
26. B. Yang, C. J. Jiang, G. Yu, Q. F. Zhuo, S. B. Deng, J. H. Wu, H. Zhang, *J. Hazard. Mater.* 299 (2015) 417-424.
27. Y. M. Wang, B. Hu, C. L. Hu, X. F. Zhou, *Mat. Sci. Semicon. Proc.* 40 (2015) 744-751.
28. Y. H. Jiang, Z. X. Hu, M. H. Zhou, L. Zhou, B. D. Xi, *Sep. Purif. Technol.* 128 (2014) 67-71.
29. Y. H. Cui, Y. J. Feng, Z. Q. Liu, *Electrochim. Acta* 54 (2009) 4903-4909.
30. Y. K. Liu, Y. J. Feng, X. W. Wu, X. G. Han. *J. Alloys Compd.* 472 (2009) 441-445.
31. Y. Liu, H. L. Liu, J. Ma, J. J. Li, *J. Hazard. Mater.* 213-214 (2012) 222-229.
32. Y. Wang, C. C. Shen, M. M. Zhang, B. T. Zhang, Y. G. Yu, *Chem. Eng. J.* 296 (2016) 79-89.
33. Y. J. Feng, Y. H. Cui, B. Logan, Z. Q. Liu, *Chemosphere* 70 (2008) 1629-1636.
34. C. R. Costa, M. R. Botta, L. G. Espindola, P. Ivi, *J. Hazard. Mater.* 153 (2008) 616-627.
35. Y. Duan, Y. Chen, Q. Wen, T. G. Duan, *J. Electroanal. Chem.* 768 (2016) 81-88.
36. F. C. Xie, Y. Xu, K. Y. Xia, C. X. Jia, P. Zhang, *Ultrason. Sonochem.* 28 (2016) 199-206.
37. M. Rivera, M. Pazos, M. Sanroman, *J. Chem. Technol. Biotechnol.* 84 (2009) 1118-1124.
38. X. L. Li, X. M. Li, W. J. Yang, X. H. Chen, W. L. Li, B. B. Luo, K. L. Wang, *Electrochim Acta* 146 (2014) 15-22.
39. X. Y. Duan, Y. Y. Zhao, W. Liu, L. M. Chang, X. Li, *J. Taiwan Inst. Chem. E.* 45 (2014) 2975-2985.
40. S. Zhao, H. Ma, M. Wang, C. Cao, J. Xiong, *J. Hazard. Mater.* 180 (2010) 86-90.